Lubricants for Rigid Magnetic Media Based upon Cyclotriphosphazenes: Interactions with Lewis Acid Sites

R. J. Waltman*

IBM Storage Systems Division, 5600 Cottle Road, San Jose, California 95193

B. Lengsfield and J. Pacansky

IBM Almaden Research Center, 650 Harry Road, San Jose, California 95120

Received May 2, 1997. Revised Manuscript Received August 4, 1997[⊗]

Lubricants such as polyperfluorinated ethers are used topically on rigid magnetic media, or computer disks, to provide a low friction interface. These materials are subject to degradation particularly in the presence of Lewis acids; however, the degradation may in part be mitigated by the addition of additives such as bis(4-fluorophenoxy)tetrakis(3-(trifluoromethyl)phenoxy)cyclotriphosphazene, $[(NP)_3(OC_6H_4CF_3)_4(OC_6H_4F)_2]$, or X-1P. This report explores how X-1P may preferentially interact with Lewis acid sites to impart protection to the host lubricant. Therefore, ab initio theoretical studies on the Lewis acid−base interactions between cyclotriphosphazene derivatives and AlF_3 are performed. The theoretical results indicate that the strongest binding between X-1P and AlF_3 is achieved when the endocyclic nitrogen atom bonds to the aluminum, providing a binding energy of the order of −55 kcal/mol. The magnitude of the binding energy indicates significant bonding as opposed to a dipole−dipole attraction. The lone pair of electrons on the phenoxy substituents also provide strong binding to AlF_3, although not to the extent the nitrogen atoms do, with binding energies near −37 kcal/mol. Binding to fluorine is considerably smaller, near −8 kcal/mol. The population analyses indicate that the preferred nitrogen interaction involves the p-orbital that contains the in-plane lone pair of electrons. A computed reaction coordinate with $[NPH_2]_3$ and AlF_3 gives every indication that the in-plane interaction is strongest and most stable on the potential energy surface. There is little desire on the part of the N_3P_3 ring itself to interact with Lewis acid sites parallel to the plane of the ring, i.e., with the p-orbitals housing the lone pair of electrons perpendicular to the plane of the ring. These orbitals instead provide weak π bonding with the phosphorus d-orbitals and are energetically well below the HOMO. The reason for the strong binding between AlF_3 and the ring nitrogen atom originates from the polar, almost zwitterionic character of the endocyclic P−N bond, which polarizes the nitrogen atom negatively. All data lead to the conclusion that if the ring nitrogen in X-1P is sterically accessible, this will be the preferred binding site.

Introduction

Bis(4-fluorophenoxy)tetrakis(3-(trifluoromethyl)phenoxy)cyclotriphosphazene, $[(NP)_3(OC_6H_4CF_3)_4(OC_6H_4F)_2]$, produced by The Dow Chemical Co. and known in the computer disk industry as X-1P, is undergoing evaluation as a topical lubricant for rigid magnetic media, or computer disks. Some attractive properties of X-1P include an extremely low vapor pressure, high thermal stability, and excellent solubility in non-CFC (chlorofluorocarbon) solvents.[1] Some data indicate that as a neat lubricant, stiction and lubricant durability are excellent.[2] However, there is also some question as to whether or not the application of X-1P on a computer disk in the 10−15 Å film thickness regime results in a uniform coverage of the disk.[2]

X-1P has also been utilized as an additive in polyperfluorinated ether (PPFE) lubricants. The X-1P additive enhances the durability of the host PPFE, in particular, the Z-DOL family of lubricants, mitigating Lewis acid-induced degradation.[3,4] However, X-1P and PPFEs are also mutually insoluble, requiring tight processing controls to optimize performance.

Despite the mixed results that presently surround the use of X-1P, one fact consistently emerges; the addition of X-1P to PPFE lubricants appears to significantly increase the durability of the host PPFE lubricant, possibly reducing the head-disk interfacial (HDI) chemistry that eventually leads to degradation of the PPFE.[3] The details of how X-1P provides such protection is speculative; it is generally believed that X-1P preferentially passivates catalytic sites on disk and slider that

⊗ Abstract published in *Advance ACS Abstracts,* September 15, 1997.

(1) Nader, B. S.; Kar, K. K.; Morgan, T. A.; Pawloski, C. E.; Dilling, W. L. *Tribol. Trans.* **1990**, *35*, 37.

(2) (a) Perettie, D. J.; Johnson, W. D.; Morgan, T. A.; Kar, K. K.; Potter, G. E.; DeKoven, B. M.; Chao, J.; Lee, Y. C.; Gao, C.; Russak, M. In *ISPS−Vol. 1, Advances in Information Storage and Processing Systems*; Adams, G. G., Bhushan, B., Miu, D., Wickert, J., Eds.; Book No. H101016, 1995. (b) Lin, J.-L.; Yates, Jr., J. T. *J. Vac. Sci. Technol.* **1995**, *A13*, 1867. (c) Yang, M.; Talke, F. E.; Perettie, D. J.; Morgan, T. A.; Kar, K. K.; DeKoven, B.; Potter, G. E. *Tribol. Trans.* **1995**, *38*, 636.

(3) Kasai, P. H.; Wheeler, P. *Appl. Surf. Sci.* **1991**, *52*, 91.

(4) Herrera-Fierro, P.; Jones, W. R.; Pepper, S. V. *J. Vac. Sci. Technol.* **1993**, *A11*, 355.

S0897-4756(97)00313-X CCC: $14.00

Table 1. Total Energies (hartrees) at HF/3-21G* and HF/6-31G* Optimized Geometries

structure	3-21G*	6-31G*
$[NPH_2]_3$ (Figure 1)	−1 183.228 790 392 (D_{3h})	−1 188.983 096 713 (D_{3h})
	−1 183.881 615 154 (D_{3h}, MP2)	
	−1 183.228 790 313 (C_1)	
$[NPH_2]_3-AlF_3$ (Figure 4a)	−1 720.880 049 701 (C_1)	
	−1 722.047 794 007 (C_1, MP2)	
$[NPH_2]_3-AlF_3$ (Figure 4b)	−1 720.900 791 473 (C_{3v})	
$[NPH_2]_3-AlF_3$ (Figure 4d)	−1 720.977 411 723 (C_1)	−1 729.510 697 153 (C_1)
$[NP(OH)_2]_3$ (Figure 5a)	−1 630.275 577 440 (C_1)	−1 638.395 988 992 (C_1)
$[NP(OH)_2]_3-AlF_3$ (Figure 5b)	−2 168.056 986 280 (C_1)	−2 178.938 019 379 (C_1)
$[NP(OH)_2]_3-AlF_3$ (Figure 5c)	−2 168.021 333 463 (C_1)	−2 178.907 641 524 (C_1)
Figure 8a	−2 518.947 476 737 (C_1)	
Figure 8b	−3 056.721 199 850 (C_1)	
Figure 8c	−3 056.689 834 743 (C_1)	
Figure 8d	−3 056.648 602 838 (C_1)	
AlF_3	−537.638 440 533 (C_1)	−540.450 451 568 (C_1)
	−538.058 281 338 (C_1, MP2)	

could otherwise interact with the PPFE lubricant and possibly initiate degradation.

In this report, ab initio theoretical studies are presented in an effort to identify the reactive sites on the X-1P molecule. As shown in the structures below, a number of potential binding sites are available; the endocyclic nitrogen, and the exocyclic oxygen, fluorine, and benzene moieties. The goal of this paper is to elucidate the role of molecular and electronic structure of X-1P and provide a rational basis for understanding their interactions with Lewis acid sites. This is best achieved by decomposing the X-1P molecule to its definitive cyclotriphosphazene structure, $[NP(H_2)]_3$, and subsequently increasing the size of the ligand to −OH and then $-OC_6H_4R$, where R is either F or CF_3, to evaluate ligand effects. The X-1P molecule is formed when the $-OC_6H_4R$ ligands, where R equals CF_3- and F−, are in a 2:1 ratio. The actual relative positions of the $-OC_6H_4CF_3$ and $-OC_6H_4F$ ligands may be unknown. Therefore, we have considered the X-1P structure shown here as a representative structure:

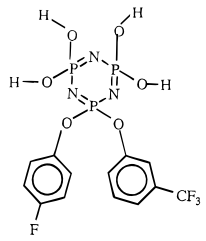

Pre-X-1P

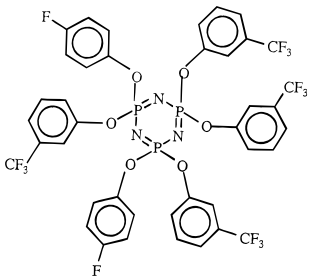

X-1P

The theoretical results indicate that the strongest binding between X-1P and AlF_3 occurs with the endocyclic nitrogen and aluminum. The bonding to nitrogen will occur with the nitrogen p-orbitals housing the lone pair of electrons that are in-plane to the cyclotriphosphazene ring. The interaction of AlF_3 with the nitrogen p-orbitals perpendicular to the plane of the ring represent complexes that are much higher in energy on the Lewis acid−base reaction coordinate. The p-orbitals housing the lone pair of electrons on the exocyclic oxygen atoms of the phenoxy substituents also provide strong binding to aluminum. Thus, steric hindrance imparted by the ligands will influence the available binding sites on X-1P.

Computational Method

Ab initio calculations were performed using the *Mulliken* computer code[5] on IBM RISC 6000 computers. Hartree−Fock (HF) and MP2 calculations were performed using both the 3-21G* and the 6-31G* basis sets.[6] d-Orbitals are included in all computations because of their importance in accurately describing phosphorus chemistry. The total energy of all computed species are summarized in Table 1. All of the structures considered here were fully optimized. The harmonic vibrational frequencies were calculated for the following structures: $[NPH_2]_3$, $[NPH_2]_3-AlF_3$, $[NP(OH)_2]_3$, and $[NP(OH)_2]_3-AlF_3$, by differentiation of the energy gradient at the optimized geometries. No imaginary frequencies were computed. The larger Pre-X-1P and X-1P molecules were fully optimized, but no frequencies were computed. We note that all optimized geometries computed here are associated with local, not necessarily global, minima. The use of these structures is not expected to mitigate against the conclusions presented in this study.

Results and Discussion

$[NPH_2]_3$: The results for the geometry optimization of $[NPH_2]_3$ are presented in Figure 1a and Table 2. The optimized structure represents a minimum on the potential energy surface with no imaginary frequencies. The most significant structural result is the planarity of the cyclotriphosphazene ring. The N−P−N−P dihedral angles are all 0°, and the P−N−P and N−P−N bond angles are 123° and 117°, at SCF/6-31G*, respectively. As seen in Table 2, the SCF/3-21G* and MP2/3-21G* results do not differ significantly. Previous crystal structure analyses of $[NP(R_2)]_3$, where R = Me, F, Cl, and Br, are indicative of rings that are planar or very nearly so.[7−10] The optimized bond lengths, angles, and dihedrals (Table 2) are similar to the values

(5) *Mulliken*, Lengsfield, B. H.; McLean, A. D.; Carter, J. T.; Replogle, E. S.; Barnes, L. A.; Maluendes, S. A.; Lie, G. C.; Rice, J. E.; Horn, H.; Gutowski, M.; Rudge, W. E.; Sauer, S. P. A.; Lindh, R.; Andersson, K.; Chevalier, T.; Widmark, P.-O.; Bouzida, D.; Pacansky, G.; Singh, K.; Gillan, C. J.; Carnevali, P.; Swope, W. C.; Liu, B. Almaden Research Center, IBM Research Division, 6500 Harry Road, San Jose, CA 95120-6099.

(6) Raghavachari, K.; Pople, J. A. *Int. J. Quantum Chem.* **1981**, *20*, 1067.

(7) Oakley, R. T.; Paddock, N. L.; Rettig, S. T.; Trotter, J. *Can. J. Chem.* **1977**, *55*, 4206.

(8) Dougill, M. W. *J. Chem. Soc.* **1963**, 3211.

(9) Bullen, G. J. *J. Chem. Soc. A* **1971**, 1450.

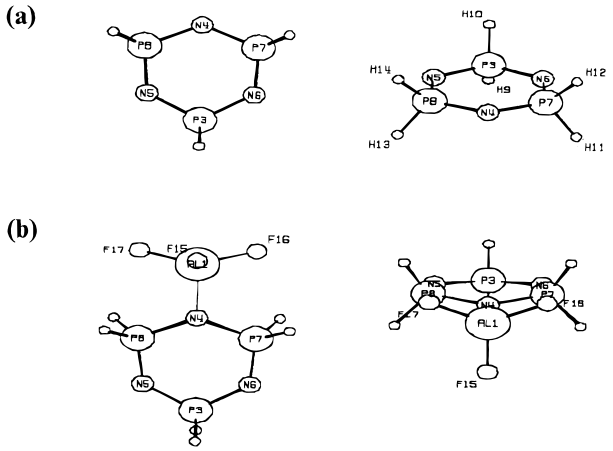

Figure 1. SCF/6-31G* optimized geometries: (a) $[NPH_2]_3$; (b) the interaction of $[NPH_2]_3$ with AlF_3.

obtained previously by Ferris et al.[11] at the SCF level of theory. Comparison of computed and experimental geometries on structurally analogous cyclotriphosphazenes (R = F, Cl, CH_3) indicate that results closest to experiment are obtained when flexible basis sets including d-orbitals are employed.[12] With the inclusion of polarization functions in the basis set, excellent theoretical structural results are obtained even at the modest 3-21G* basis set. For $[NPH_2]_3$, the use of correlated wave functions (MP2) provides only modest changes to the SCF geometries. The P−N and P−H bond lengths are only approximately 1% longer at MP2/3-21G*, and this lengthening appears to be in the correct direction based upon an extrapolation of Haddon's data.[12] Hence, as concluded by Ferris et al., the inclusion of d-orbitals in the basis set appears to have the most significant effect in describing the structure and bonding of cyclotriphosphazenes. The bond order data, also summarized in Table 2, reveal in all cases a value of approximately 1.3 for the P−N bond, indicative of a relatively weak π double-bond character.

Molecular orbital plots (SCF/6-31G*) are presented in Figure 2 for the π' (in-plane) and π (out-of-plane) contours. The π' orbital contour, which represents the highest occupied molecular orbital (HOMO), reveals that the inclusion of the d-orbitals significantly increases the in-plane nitrogen lone-pair interactions, thereby stabilizing the planar ring conformation despite the lack of aromaticity (see bond order data). The π orbital contour (3HOMO) is dominated by the lone pair of electrons perpendicular to the ring for each of the nitrogen atoms. d-orbital interactions in the π orbital become important as the electronegativity of the substituent increases.[11]

The partial atomic charges are summarized in Table 3. Both Mulliken charges and charges computed from a fit to the electrostatic potential field (ESP) surrounding the molecule are presented. The ESP charges were constrained to reproduce the dipole moment of the molecule, 0 D. If the ESP charges at the MP2 geometries are considered to be "best" results, then the Mulliken charges at 3-21G* and 6-31G* provide comparable data. The ESP charges computed at 3-21G* and 6-31G* geometries are considerably larger in magnitude and reflect the highly polar nature of the P−N bond. The Mulliken charges at 3-21G* and 6-31G* indicate that the nitrogen atom has accumulated an excess negative charge of approximately -0.9 e^-, while the phosphorus atoms are highly positively charged, approximately 1.0 e^-, resulting in a highly polarized P−N bond.

As an indication for the preferred interaction sites in $[NPH_2]_3$ with an electrophile, the SCF/3-21G* electrostatic potential surface for the molecule is presented in Figure 3, for a 6.3 kcal/mol isosurface. The region of negative potential, colored blue in the figure, is evident as the nitrogen lone pairs of electrons, spatially protruding primarily out of the plane of the ring. An electrophile may therefore be expected to approach the in-plane nitrogen lone pair of electrons in $[NPH_2]_3$.

$[NPH_2]_3$−AlF_3: The results of the previous section identified the polar nature of the P−N bond. From a consideration of the molecular orbital plots and electrostatic potential field, it became clear of the availability of the in-plane lone pair of electrons on nitrogen for bonding with Lewis acidic centers such as aluminum in AlF_3. Experimental data provide evidence for the formation of 1:1 adducts of aluminum Lewis acids with structurally analogous cyclotriphosphazenes.[13] In these studies, we employ AlF_3 as a model for a Lewis acid surface sites for several reasons. First, XPS studies on the wear tracks of slided disks reveal the presence of metal fluorides that are thought to induce the degradation of perfluorinated ether lubricants.[14] Second, AlF_3 has comparatively few electrons and is a closed shell, rendering the computational studies more tractable. The actual surface may be more ionic and possibly more coordinatively unsaturated than the bulk.[15] The use of AlF_3 is not expected to mitigate against the conclusions presented in this study.

We now present results from a theoretical study of Lewis acid−base complex formation between $[NPH_2]_3$ and AlF_3. The individual starting geometries in the complex were previously optimized at SCF/3-21G*. The reaction coordinate as a function of energy is presented in Figure 4. Two possible interactions between $[NPH_2]_3$ and AlF_3 were considered. In one trajectory, the aluminum atom in AlF_3 approaches an endocyclic nitrogen of $[NPH_2]_3$ in the ring plane. In the other trajectory, the $[NPH_2]_3$ ring sits atop AlF_3 such that the $[NPH_2]_3$ ring sits parallel to the AlF_3 surface, with the aluminum center equidistant to all three endocyclic nitrogen atoms. From the discussions presented above on the electrostatic potentials and molecular orbital contours for $[NPH_2]_3$, it is gratifying to see in Figure 4 that the Lewis acid interaction providing the lowest total energy for the $[NPH_2]_3$−AlF_3 complex is the one whereby the aluminum atom in AlF_3 interacts strongly with the in-plane nitrogen lone pair of electrons, providing the (local) minimum structure 4d. Conversely, when the plane of the cyclotriphosphazene ring is parallel to the AlF_3 surface, as shown in the optimized structures 4a and 4b, the complexes do not correspond to minima on the potential surface, as imaginary frequencies are

(10) Zoer, H.; Koster, D. A.; Wagner, A. J. *Acta Crystallogr.* **1969**, *A25*, S107.
(11) Ferris, K. F.; Friedman, P.; Friedrich, D. M. *Int. J. Quantum Chem.* **1981**, *22*, 207.
(12) Haddon, R. C. *Chem. Phys. Lett.* **1985**, *120*, 372.
(13) Allcock, H. R. *Chem. Rev.* **1972**, *72*, 315.
(14) Mori, S.; Morales, W. *Wear* **1989**, *132*, 111.
(15) Williams, S. D.; Harper, W.; Mamantov, G.; Tortorelli, L. J.; Shankle, G. *J. Comput. Chem.* **1996**, *17*, 1697.

Table 2. Optimized Geometries and Bond Order (BO) for $[NPH_2]_3$ with D_{3h} Point Group

basis	P−N	P−H	P−N−P	N−P−N	H−P−N	N−P−N−P	H−P−N−P
3-21G*	1.590	1.385	126.00	114.00	110.27	0.00	±124.66
BO	1.299	0.867					
MP2/3-21G*	1.611	1.402	122.75	117.25	109.48	0.00	±125.47
BO	1.273	0.805					
6-31G*	1.594	1.387	123.44	116.56	109.51	0.00	±124.97
BO	1.263	0.900					

Table 3. Computed Mulliken and Electrostatic Potential (ESP) Partial Atomic Charges for $[NPH_2]_3$ with D_{3h} Point Group

	Mulliken			ESP		
basis	P	N	H	P	N	H
3-21G*	1.036	−0.913	−0.062	1.658	−1.288	−0.185
MP2/3-21G*	0.785	−0.711	−0.037	1.249	−0.994	−0.123
6-31G*	1.053	−0.925	−0.064	1.514	−1.217	−0.150

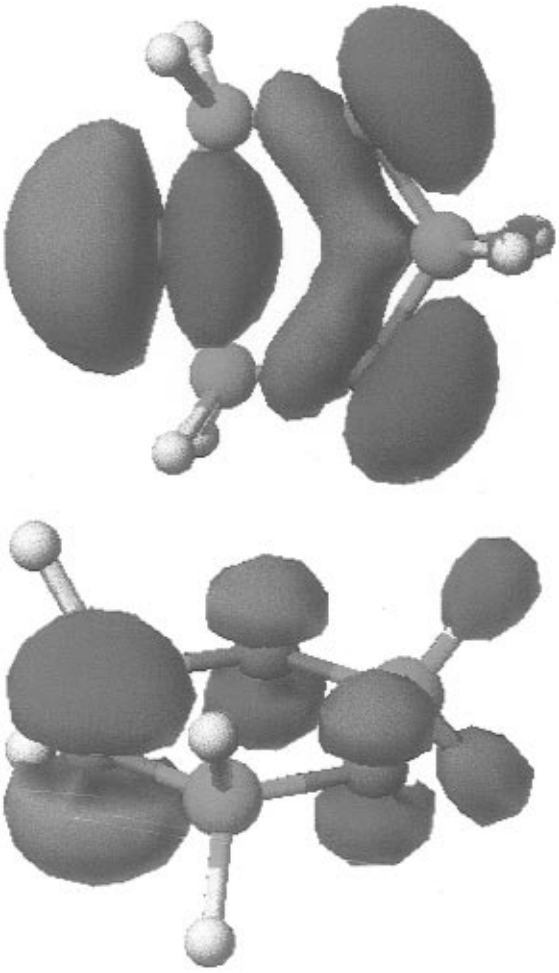

Figure 2. SCF/6-31G* molecular orbital plots. Top: HOMO. Bottom: 3HOMO.

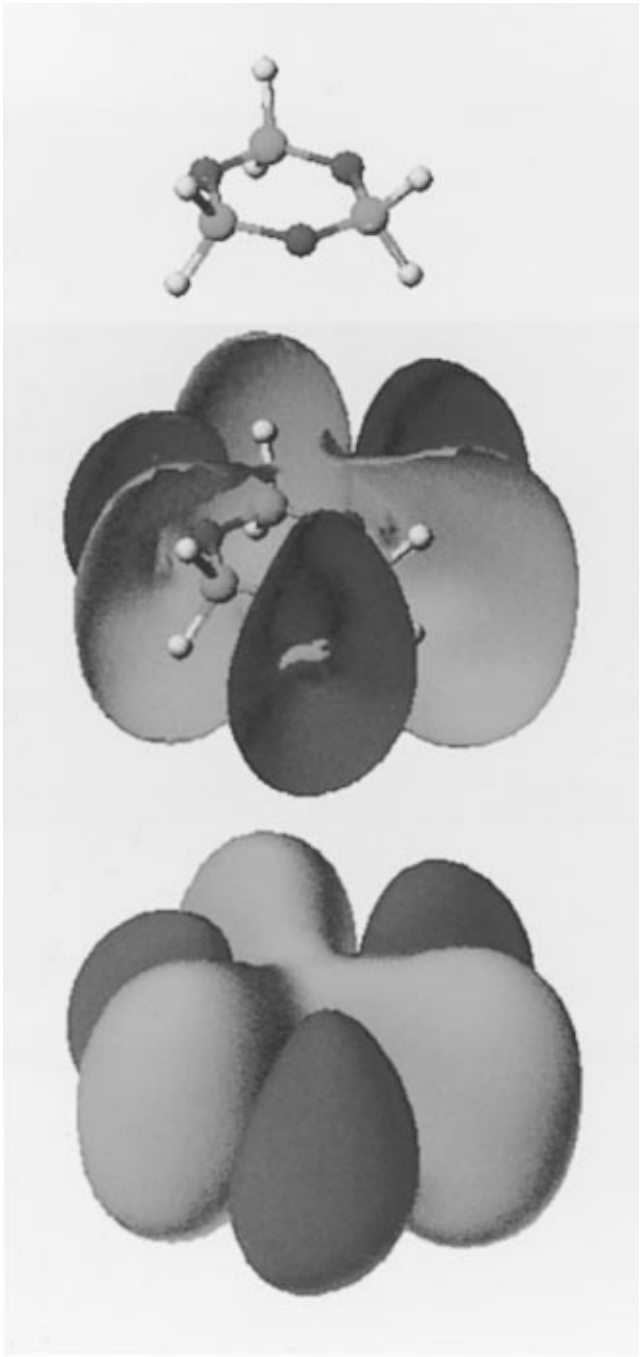

Figure 3. SCF/3-21G* electrostatic potential surface for $[NPH_2]_3$ at 6.3 kcal/mol isosurface energy. The blue regions are negative, and the red regions are positive.

computed for both structures associated with out-of-plane ring deformations involving the ring nitrogens and aluminum. In structure 4a, the cyclotriphosphazene ring was constrained to be planar and in structure 4b, only C_{3v} symmetry was imposed. As a matter of interest, the distance between the center of the Al atom and the plane of the ring are 3.1 and 2.3 Å, respectively, for structures 4a and b, respectively. When the C_{3v} symmetry is relaxed in 4b and the complex allowed to optimize freely, the resultant geometry is 4d. Along this reaction coordinate, a structure 4c is also identified in Figure 4. The structure 4c is not optimized but is instead a point along the reaction coordinate which merely serves to pictorially connect the "docking" of the cyclotriphosphazene ring to the AlF_3 surface from its initially ring plane-parallel structure shown in Figure 4b to its final, in-plane interaction in Figure 4d.

The optimized geometry for structure 4d is presented in Figure 1b and Table 4. This structure is a minimum on the potential energy surface with no computed

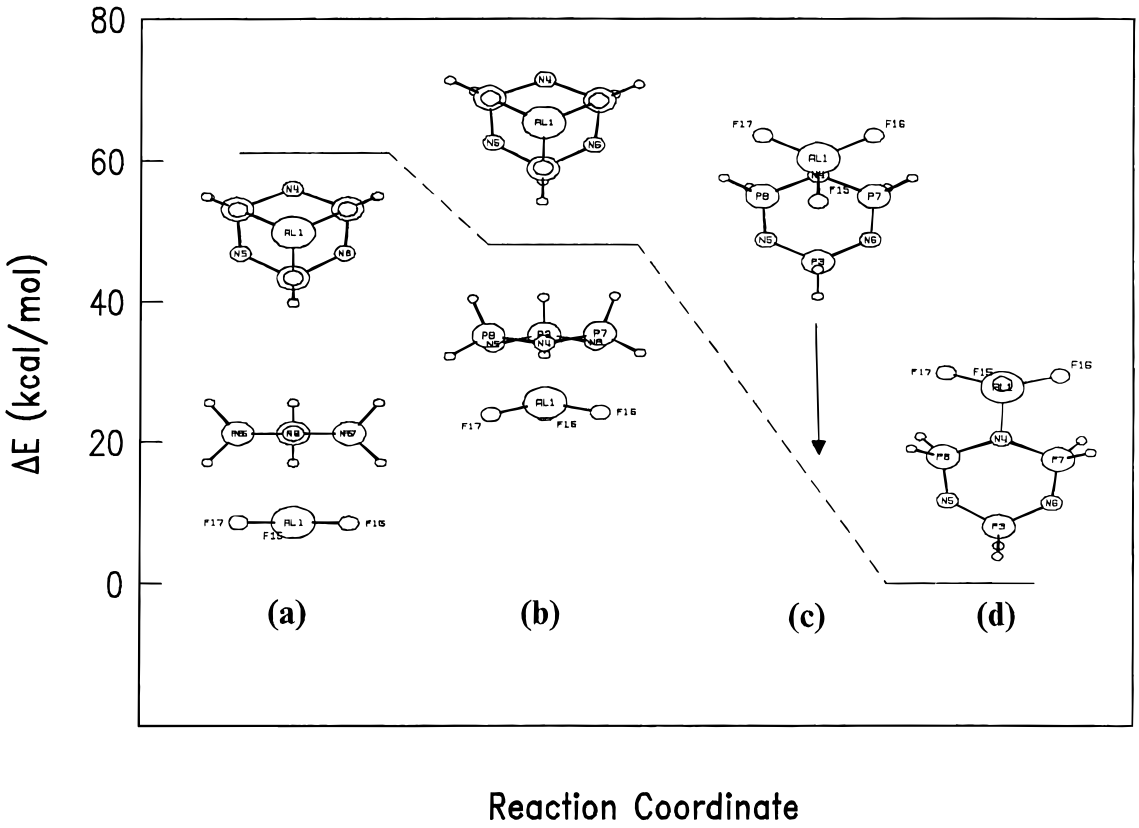

Figure 4. SCF/3-21G* reaction coordinate for the interaction between $[NPH_2]_3$ and AlF_3. Two views of the same complex are shown for (a) and (b). The free optimization of either complexes (a) and (b) lead to the in-plane interacting complex (d). The complex (c) is a single point along the reaction coordinate from (b) to (d) and is not a local minimum.

Table 4. HF/3-21G* Optimized Geometry for Structure 4d (Figure 4), $[NPH_2]_3-AlF_3$, with C_1 Point Group (BO Is the Bond Order)

bond	length	BO	bond	angle	bond	dihedral
N4−P7	1.647	1.004	P8−N4−P7	124.23	Al1−N4−P7−N6	172.75
N6−P7	1.574	1.360	N4−P7−N6	111.78	N4−P7−N6−P3	6.61
P3−N6	1.588	1.266	P7−N6−P3	128.80	P7−N6−P3−N5	2.84
Al1−N4	1.901	0.438	N6−P3−N5	112.30	N6−P3−N5−P8	−3.43
Al1−F15	1.642	0.950	Al1−N4−P7	117.40	F15−Al1−N4−P7	−94.84
Al1−F16	1.655	0.840	F15−Al1−N4	112.76	F16−Al1−N4−P7	23.61

imaginary frequencies. Several changes in the ring skeletal geometry are evident as a result of the interaction of N4 with AlF_3. First, the P−N4 bond distances increase dramatically from 1.590 (Table 1) to 1.647 Å. Second, the ring is slightly distorted from planarity (Table 4). The distance between the Al1 and N4 atomic centers is very short, 1.901 Å, typical of Al−N bonding.[16] A bond order of 0.44 is computed for the same Al−N bond (Table 4). These data indicate that the Lewis acid is chemically bound to the cyclotriphosphazene ring and not simply interacting via weaker forces such as a dipole−dipole attraction.

The binding energy for the aluminum−nitrogen couple in the $[NPH_2]_3-AlF_3$ complex is computed to be −67 and −47 kcal/mol at HF/3-21G* and /6-31G*, respectively, as summarized in Table 5. The binding energy is defined here as the difference between the total energy of the complex and the initial reactants, corrected for zero-point energy contributions. The binding energy for the aluminum−nitrogen Lewis acid−base pair is quite substantial, regardless of the employed basis set, and considerably larger than the −9 kcal/mol (HF/6-31G*) computed for the aluminum−oxygen Lewis acid−base couple between CF_3OCF_3 and AlF_3.[17] As an indication for the accuracy of the calculations, we report that a thermal desorption study of polyperfluorinated ethers on metal substrates have produced an interaction or binding energy of 8−10 kcal/mol per ether linkage.[18]

Table 5. Some Computed Binding Energies for Lewis Acid−Base Pairs (All Values Corrected for Zero-Point Energies (ZPE) Are Included)

	HF/3-21G*		HF/6-31G*	
AlF_3 complexes with	ZPE	no ZPE	ZPE	no ZPE
CF_3OCF_3 ether oxygen			−9.1[17]	−9.9[17]
$[NPH_2]_3$ ring nitrogen	−67.2	−69.1	−46.9	−48.4
	−65.6[a]	−67.7[a]		
$[NP(OH)_2]_3$ ring nitrogen	−86.5	−89.7	−55.1	−57.5
$NP(OH)_2]_3$ oxygen	−64.0	−67.3	−36.2	−38.4
Figure 8b ring nitrogen	−82.4	−84.9		≃−54[b]
Figure 8c oxygen		−65.2		≃−34[b]
Figure 8d fluorine		−39.3		≃−8[b]

[a] Energies from fully optimized MP2/3-21G* structures; no imaginary frequencies. [b] Estimated HF/6-31G* energies obtained by uniformly subtracting 31 kcal/mol from the corresponding HF/3-21G* energies. The 31 kcal/mol correction factor was obtained by the average difference between binding enegies at HF/3-21G* and HF/6-31G* for $[NP(OH)_2]_3$ nitrogen and oxygen interactions with AlF_3.

(16) Mole, T.; Jeffery, E. A. *Organoaluminum Compounds*; Elsevier Publishing Co.: New York, 1972; p 237−238.

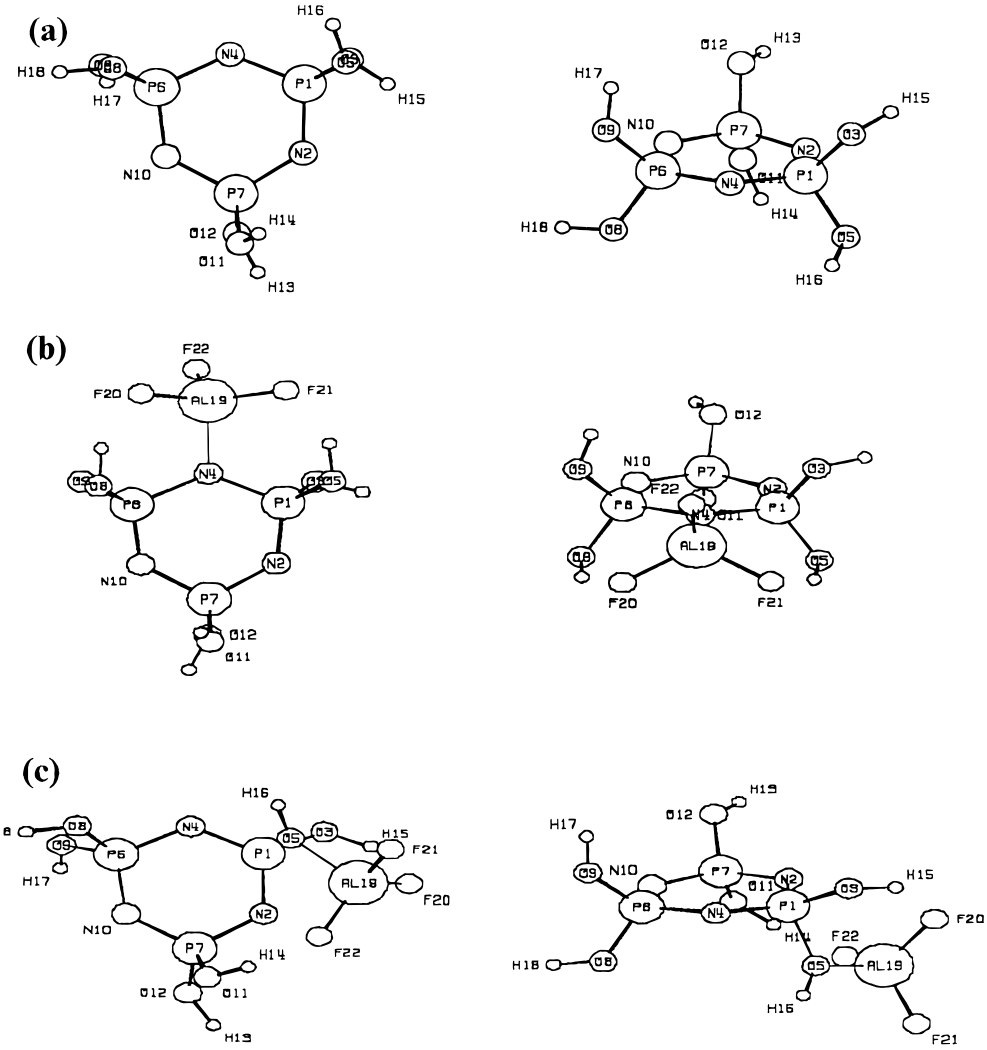

Figure 5. SCF/6-31G* optimized geometries: (a) $[NP(OH)_2]_3$; (b) the interaction of AlF_3 with an endocyclic nitrogen atom; (c) the interaction of AlF_3 with a hydroxy oxygen atom.

Table 6. Optimized Geometries and Bond Order (BO) for $[NP(OH)_2]_3$ with C_1 Point Group

bond	3-21G*	BO	6-31G*	BO
P−N	1.574 ± 0.004	1.312 ± 0.013	1.579 ± 0.005	1.279 ± 0.011
P−O	1.580 ± 0.004	1.026 ± 0.001	1.589 ± 0.004	1.021 ± 0.013
O−H	0.966 ± 0.001		0.951 ± 0.001	
P−N−P	126.93 ± 1.11		123.81 ± 1.10	
N−P−N	112.99 ± 1.04		115.91 ± 1.13	
N−P−O	110.51 ± 2.09		109.69 ± 2.74	
P1−N4−P6−N10		−5.02	−9.00	
N4−P6−N10−P7		3.22	6.91	
P6−N10−P7−N2		0.98	0.86	
N10−P7−N2−P1		−4.27	−7.37	
P7−N2−P1−N4		2.81	5.51	
N2−P1−N4−P6		2.36	3.24	
P−N−P−O	±(124.55 ± 5.34)		±(124.90 ± 8.56)	
dipole moment, D	1.75		2.01	

This value compares favorably with the computed binding energy of the CF_3OCF_3 and AlF_3 Lewis acid−base complex at the HF/6-31G* level of theory (Table 5). Similar binding energies are observed experimentally for polyperfluorinated ethers on amorphous carbon.[19] As a further evaluation of the computed binding energy for the $[NPH_2]_3$−AlF_3 complex, we have also fully optimized the $[NPH_2]_3$−AlF_3 complex, and the individual reactants, at the MP2/3-21G* level of theory, to determine the magnitude of the error caused by a lack of explicit correlation treatment at the SCF level of theory. The binding energy for the aluminum−nitrogen Lewis acid−base pair at MP2/3-21G* is −66 kcal/mol, only 1 kcal/mol smaller than the corresponding binding energy at HF/3-21G*, representing an error of only a few percent. We conclude from these studies that the

(17) Pacansky, J.; Waltman, R. J. *J. Fluor. Chem.* **1997**, *83*, 41.
(18) Meyers, J. M.; Gellman, A. J. *Tribol. Lett.* **1996**, *2*, 47.
(19) Perry, S. S.; Somorjai, G. A. Mate, C. M.; White, R. *Tribol. Lett.* **1995**, *1*, 47.

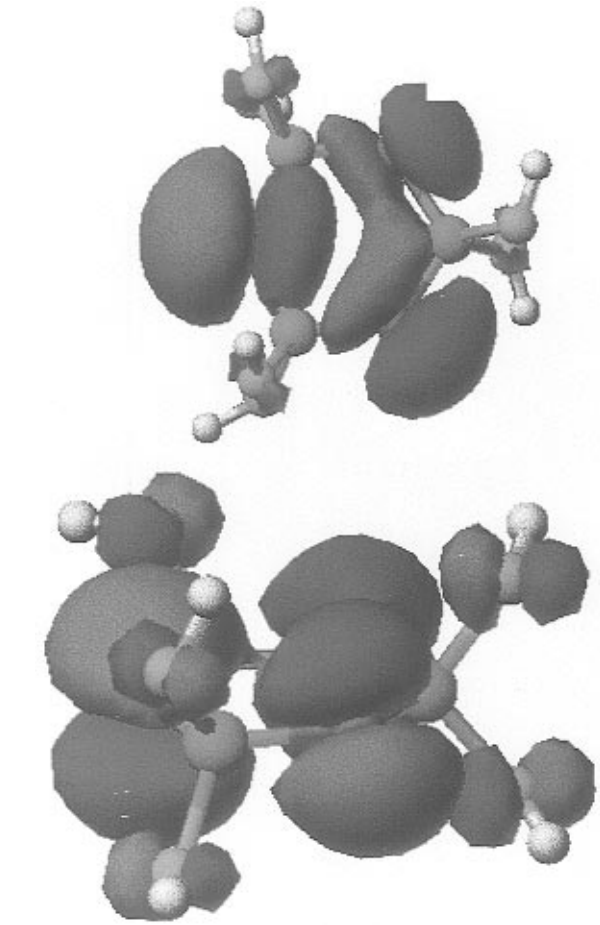

Figure 6. SCF/6-31G* molecular orbital plots. Top: HOMO. Bottom: 2HOMO.

computed binding energies converge at the SCF/6-31G* level of theory for the systems under consideration, and are similar in magnitude to experimentally available data. The 3-21G* binding energies are approximately 20 kcal/mol higher than at 6-31G* for the $[NPH_2]_3-AlF_3$ complex.

$[NP(OH)_2]_3$: The results for the geometry optimization of $[NP(OH)_2]_3$ are presented in Figure 5a and Table 6. The optimized structure is a (local) minimum on the potential energy surface with no imaginary frequencies. With OH ligands on each phosphorus atom, the planarity of the cyclotriphosphazene ring is slightly compromised, with P−N−P−N and N−P−N−P dihedral angles in the ±7° range. The computed dipole moment is 1.8−2.0 D, consistent for cyclotriphosphazene rings that develop a slight pucker.[13] The P−N bond distance is observed to decrease from 1.59 (Table 2) to 1.57−1.58 Å, due to the increased electronegativity of the O(H) ligand. Apart from these major changes in geometry, the other optimized bond lengths and angles are similar to $[NPH_2]_3$ where the structures are similar.

Molecular orbital plots for $[NP(OH)_2]_3$, presented in Figure 6, identify the predominance of the cyclotriphosphazene ring π' (in-plane) in the HOMO. The oxygen lone pairs contribute to the 2HOMO, which lies 0.12 eV below the HOMO. The molecular orbitals dominated by the oxygen lone pairs are buried 1.6 eV below the HOMO, beginning at the 4HOMO.

The partial atomic charges are computed as follows. At HF/3-21G*: P = +1.566 e^-; N = −0.973 e^-; O = −0.732 e^-; and H = +0.435 e^-. At HF/6-31G*: P = +1.461 e^-; N = −0.905 e^-; O = −0.768 e^-; and H = +0.491 e^-. The Mulliken charges at 3-21G* and 6-31G* indicate that the phosphorus atoms have acquired a considerable positive charge, approximately 1.5 e^-, due to the OH ligand on phosphorus, compared to approximately 1.0 e^- for a hydrogen ligand. One interpretation is that the P−N bonds become even more zwitterionic with greater ligand electronegativity.

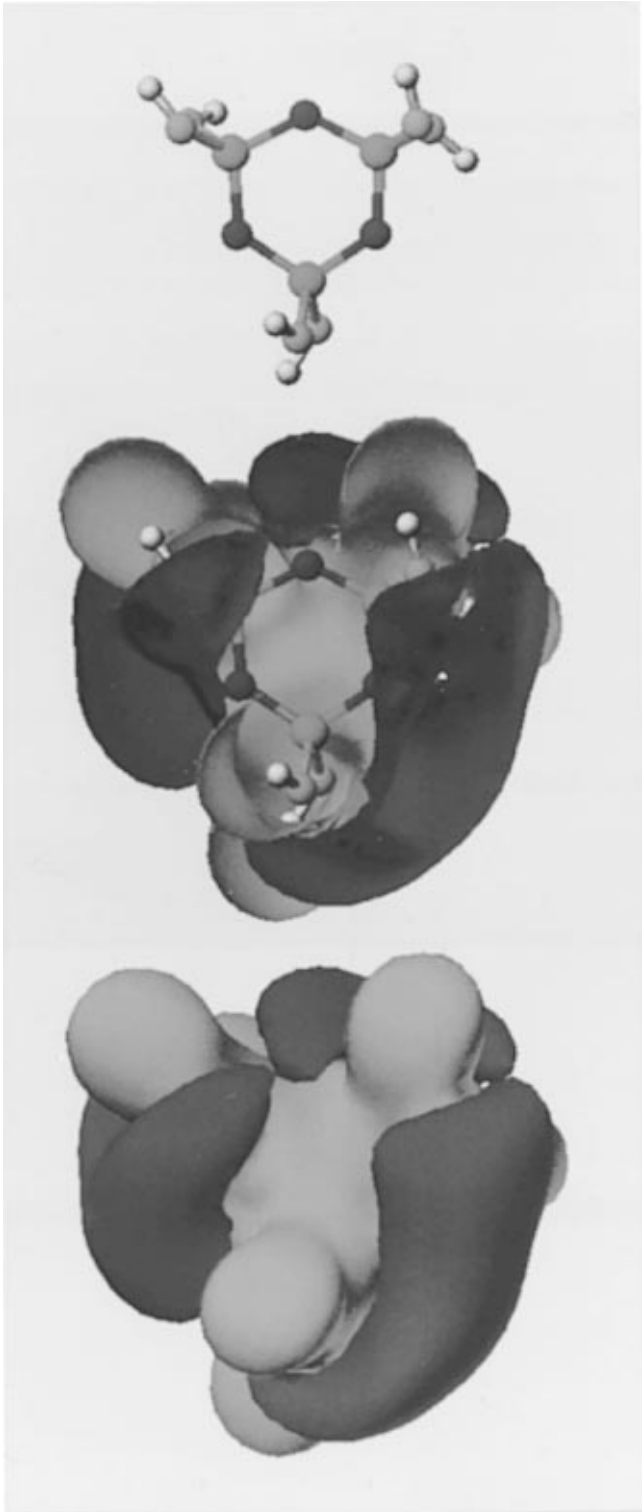

Figure 7. Electrostatic potential surface for $[NP(OH)_2]$ at 18.8 kcal/mol isosurface energy. The blue regions are negative, and the red regions are positive.

As an indication for the preferred interaction sites in $[NP(OH)_2]_3$, the electrostatic potential surface for the

Table 7. Optimized Geometries and Bond Orders (BO) for $[NP(OH)_2]_3-AlF_3$ (See Figure 5a) with C_1 Point Group

	3-21G*		6-31G*	
bond	length	BO	length	BO
N4−P	1.644 ± 0.008	0.970 ± 0.033	1.643 ± 0.007	0.982 ± 0.027
N−P	1.558 ± 0.011	1.317 ± 0.076	1.568 ± 0.013	1.329 ± 0.070
P−O	1.566 ± 0.009	1.069 ± 0.051	1.574 ± 0.008	1.060 ± 0.032
N4−Al19	1.896	0.480	1.949	0.468
N4−P1−N2−P7	4.62		10.91	
Al19−N4−P1−N2	172.95		172.01	
P1−N2−P7−N10	−5.88		−12.49	
N2−P7−N10−P6	0.43		0.16	
P7−N10−P6−N4	4.82		11.25	
N10−P6−N4−P1	−6.02		−12.47	

Table 8. Optimized Geometries and Bond Orders (BO) for $[NP(OH)_2]_3-AlF_3$ (See Figure 5b) with C_1 Point Group

	3-21G*		6-31G*	
bond	length	BO	length	BO
P1−O5	1.694	0.600	1.702	0.551
N−P	1.572 ± 0.020	1.286 ± 0.098	1.577 ± 0.018	1.309 ± 0.083
P−O	1.567 ± 0.009	1.072 ± 0.033	1.575 ± 0.008	1.066 ± 0.019
O5−Al19	1.860	0.389	1.915	0.322
N4−P1−N2−P7	−15.51		−20.52	
Al19−O5−P1−N4	159.96		164.74	
P1−N2−P7−N10	8.54		10.76	
N2−P7−N10−P6	−0.95		−2.33	
P7−N10−P6−N4	0.63		3.05	
N10−P6−N4−P1	−7.73		−12.05	

molecule is presented in Figure 7 for an isosurface energy of 18.8 kcal/mol. The presence of the OH ligands provides an interesting result, namely, that the ligands extend the region of negative potential and spatially "connect" the nitrogen and oxygen lone pairs of electrons providing a relatively large region of negative potential for an incoming electrophile. Moreover, the electrostatic potential surface takes into account all of the electrons in the molecule; therefore, the lone pair of electrons on the oxygen atom of the OH groups are viable reaction sites in addition to the endocyclic nitrogen atoms.

$[NP(OH)_2]_3-AlF_3$: The results in the previous section identified the availability for bonding with Lewis acidic centers of the in-plane lone pair of electrons on the nitrogen atoms of the cyclotriphosphazene ring, and the lone pair of electrons on the oxygen atom of the OH ligands. Hence, we consider next structures where the Lewis acid−base coupling with AlF_3 occurs with these atoms. The optimized geometries for both complexes of $[NP(OH)_2]_3$ with AlF_3 are presented in Figure 5b, c, and the relevant optimized structural parameters are summarized in Tables 7 and 8. Both structures are (local) minima on the potential energy surface with no computed imaginary frequencies. The changes induced in the geometry of the cyclotriphosphazene ring as a result of the aluminum−nitrogen couple (Figure 5b) are similar to the previously discussed $[NPH_2]_3-AlF_3$ complex (Figure 1b), where the structures are similar. Thus, there is a lengthening of the P−N4 bonds adjacent to the Lewis acid−base interaction site, from the nominal 1.590 to 1.643 Å. However, compared to $[NPH_2]_3-AlF_3$, the cyclotriphosphazene ring is considerably more distorted from planarity with the ring dihedral angles ±12°, at 6-31G*. This is attributed to the strong binding of the ring nitrogen to aluminum, causing additional ring distortion to sterically accommodate the AlF_3 surface. Close contacts are observed to develop between the aluminum atom and the phosphorus atoms P1 and P6, 3.1 Å, and between the oxygen and fluorine pairs O8 and F20, and O5 and F21, 2.7 Å. The aluminum atom is approximately 8° below the N4−P1−N2 plane. The distance between the Al1 and N4 atomic centers is 1.949 angstrom at HF/6-31G*, and the corresponding bond order is 0.47. The bond distance is slightly longer than the previously computed aluminum−nitrogen bond in $[NPH_2]_3-AlF_3$, due to the steric contacts that have developed here with the OH ligands.

The optimized $[NP(OH)_2]_3-AlF_3$ aluminum−oxygen coupled complex (Figure 5c) indicates that the cyclotriphosphazene ring geometry is largely unperturbed from $[NP(OH)_2]_3$ (Figure 5a) because the aluminum−oxygen interaction occurs outside the ring. There is an increase in the P1−O5 distance from 1.58 to 1.70 Å due to the aluminum−oxygen interaction. The P1−O5 bond order decreases significantly from 1.1 to 0.6; one interpretation is that the formation of the aluminum−oxygen bond has reduced the phosphorus d-orbital interaction with the cyclotriphosphazene ring. The distance between O5 and Al19 is only 1.92 Å, with an appreciable bond order of 0.32 at HF/6-31G*. This bond distance is close to the 1.9 Å normally found in Al−O bonds.[16]

The binding energy for the coupling of aluminum to nitrogen and oxygen atoms in the $[NP(OH)_2]_3-AlF_3$ complexes are computed to be −55 and −36 kcal/mol at HF/6-31G* theory, respectively, for Figures 5b,c, respectively, as summarized in Table 5. The theoretical results indicate that the aluminum−nitrogen couple is considerably stronger than the aluminum−oxygen interaction. However, the binding of AlF_3 is strong regardless of whether or not the ring nitrogen atoms or the ligand oxygen atoms are involved.

Pre-X-1P: The optimized geometry for Pre-X-1P is presented in Figure 8a. The optimized structure is a local minimum on the potential energy surface with no computed imaginary frequencies. In this structure, we have replaced two of the OH ligands in $[NP(OH)_2]_3$ with fluorophenoxy and trifluorophenoxy substituents (see Introduction). The impact of these large substituents on the geometry of the cyclotriphosphazene ring itself

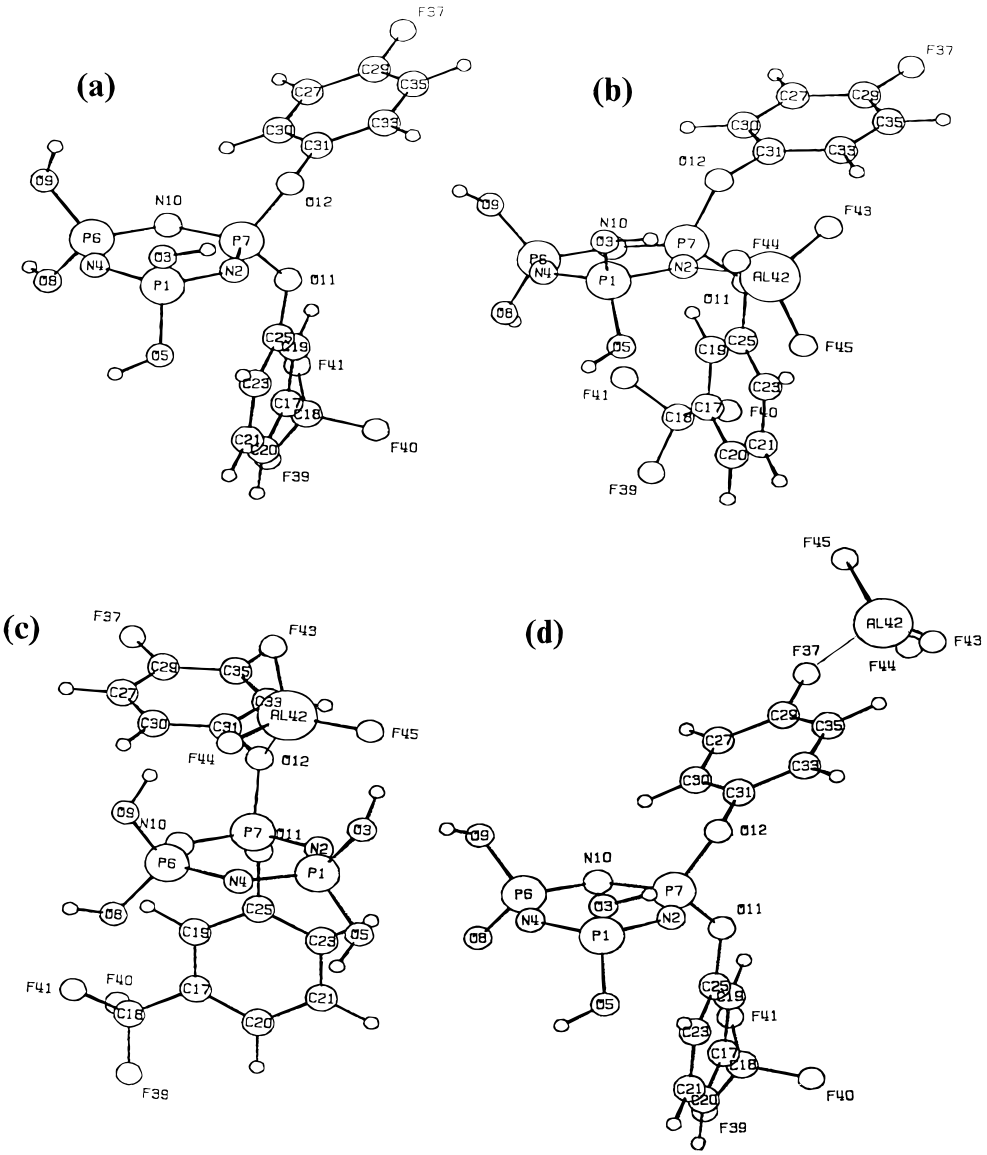

Figure 8. SCF/3-21G* optimized geometries: (a) Pre-X-1P; (b−d) the interaction of AlF_3 with an endocyclic nitrogen, a phenoxy oxygen atom, and a terminal fluorine atom, respectively.

is minimal, and hence no extensive reiteration is necessary here on the optimized geometries.

The molecular orbital plots, presented in Figure 9, indicate a re-ordering of the molecular orbitals and corresponding energies compared to $[NPH_2]_3$ and $[NP(OH)_2]_3$. The HOMO is no longer composed of the π' in-plane nitrogen lone pairs of electrons of the cyclotriphosphazene rings; instead, the first four HOMOs are directly attributed to the phenoxy substituents. The first two HOMOs contain contributions from the lone pairs of electrons on the oxygen atom and the π electrons in the benzene rings. The difference is significant from a frontier orbital perspective since the implication is that these sites are more readily available for chemistry than the cyclotriphposphazene ring. The molecular orbitals containing the in-plane nitrogen lone pairs are 1.53 eV beneath the HOMO, at the 5HOMO. An interpretation is that the in-plane nitrogen atoms are less available for chemistry. However, we would be remiss in ignoring the strong binding that develops between the cyclotriphosphazene ring nitrogen and the aluminum Lewis acid site in the previous systems investigated. As further consideration, the electrostatic potential field surrounding Pre-X-1P is presented in Figure 10. Here, the isosurface is 6.3 kcal/mol, and the regions of negative potential include the nonbonded electrons on the ring nitrogens, phenoxy oxygens and fluorines, and also the benzene π electrons. At the 6.3 kcal/mol isosurface, an electrophile could interact with all of these regions of negative potential (as long as they are sterically accessible). When the isosurface is increased to 18.8 kcal/mol, the more strongly negative regions are identified, and these include the nonbonded electrons on the ring nitrogen atoms, and the phenoxy oxygen and fluorine atoms. The benzene π electrons are no longer evident at the 18.8 kcal/mol isosurface. At a 31.4 kcal/mol isosurface, minima are located on the oxygen and nitrogen lone pairs of electrons. Hence, the docking of Pre-X-1P on the AlF_3 surface may be expected to occur most strongly with the cyclotriphosphazene nitrogen and/or the phenoxy oxygen atoms.

Pre-X-1P−AlF_3: The results of the previous section identified potentially strong binding of Lewis acids with the in-plane lone pair of electrons on the nitrogen atoms of the cyclotriphosphazene ring, and the lone pair of electrons on the oxygen atoms of the phenoxy ligands;

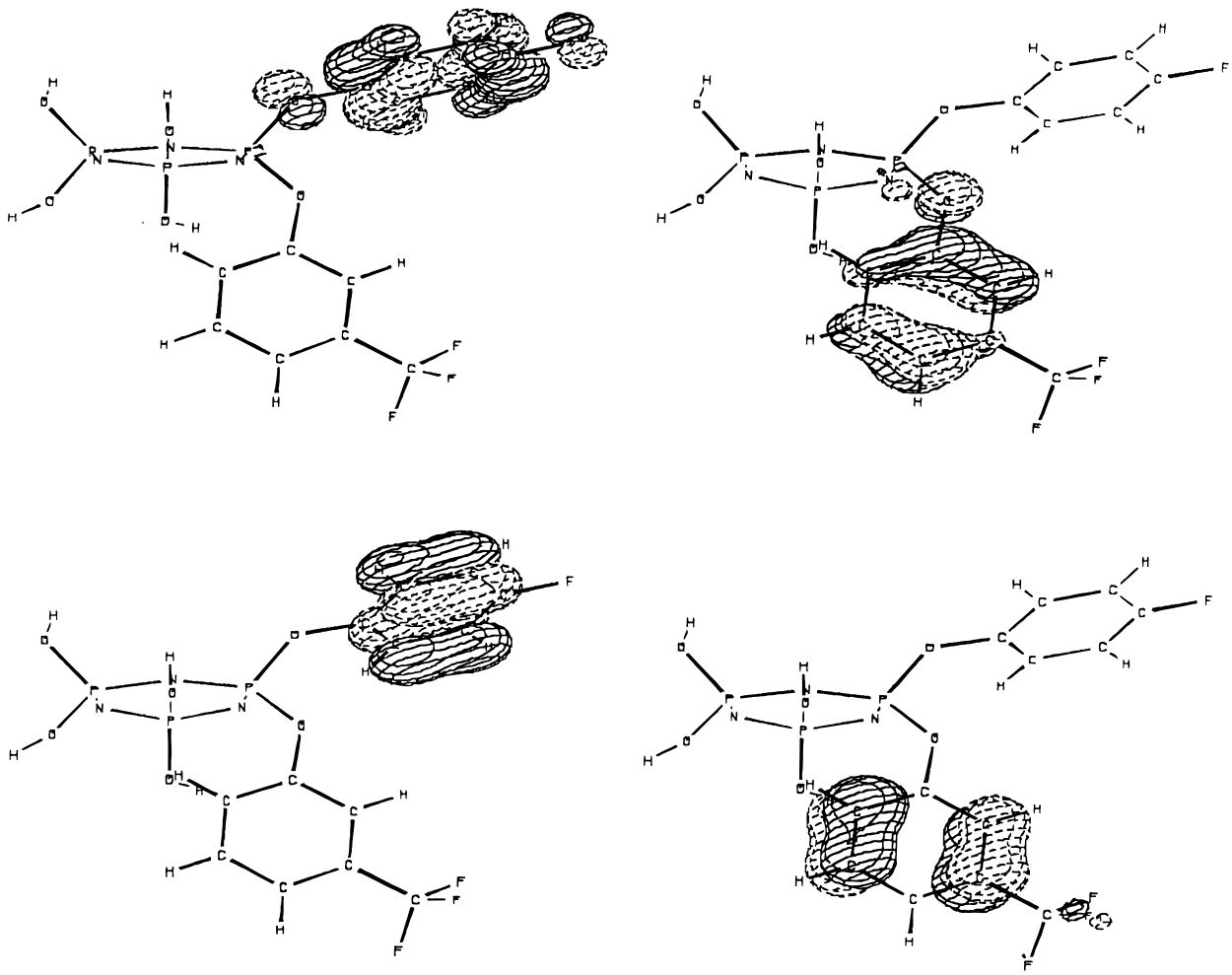

Figure 9. SCF/3-21G* molecular orbital plots. Top left: HOMO. Top right: 2HOMO. Bottom left: 3HOMO. Botom right: 4HOMO.

relatively weaker binding was expected with fluorine atoms and the benzene π system. From a frontier orbital perspective, the phenoxy oxygen lone pairs of electrons are available for chemistry. Some possible Lewis acid interactions with AlF_3 are now considered, based upon these results, and the optimized geometries for the complexes considered are presented in Figure 8b− d. No imaginary frequencies were computed for Figure 8b. The complexes in Figure 8c,d were fully optimized, but no frequencies were computed. The changes induced in the geometry of the cyclotriphosphazene ring as a result of the aluminum−nitrogen couple (Figure 8b) are similar to the previously discussed $[NP(OH)_2]_3-AlF_3$ complex (Figure 5b) where the structures are similar. Thus, there is a lengthening of the P−N2 bonds adjacent to the Lewis acid−base interaction site, from the nominal 1.590 to 1.639 Å. Close contacts are observed to develop between the aluminum atom and the phosphorus atoms P1 and P7, 3.1 Å, and between the oxygen and fluorine pairs O3 and F44, and O12 and F33, 2.5 and 3.0 Å, respectively. The distance between the Al1 and N4 atomic centers is 1.908 Å and the bond order is 0.47.

The optimized Pre-X-1P−AlF_3 aluminum−oxygen coupled complex (Figure 8c) indicates that the cyclotriphosphazene ring geometry is largely unperturbed from $[NP(OH)_2]_3$ (Figure 5a). There is an increase in the P7−O12 distance from 1.58 to 1.68 Å due to the aluminum−oxygen interaction. The accompanying P7−O12 bond order decreases considerably from 1.1 to 0.6, as observed previously for $[NP(OH)_2]_3-AlF_3$ (Figure 5c). The distance between O12 and Al42 is only 1.87 Å, with a computed bond order of 0.39 at HF/6-31G*. This Al−O bond is considerably shorter than the previous Al−O bond length of 1.92 Å computed for $[NP(OH)_2]_3-AlF_3$ (Figure 5c) and is indicative of strong aluminum−oxygen binding.

The binding energy for the coupling of aluminum to nitrogen in the Pre-X-1P−AlF_3 complex is computed to be −85 kcal/mol, at HF/3-21G*. The large size of the molecule precludes a full optimization at HF/6-31G* at this time; however, the computed binding energies for the $[NP(OH)_2]_3-AlF_3$ system gives us a correction factor of approximately 31 kcal/mol; see Table 5. Employing this uniform correction factor to relate HF/3-21G* binding energies to HF/6-31G*, the binding energy for the aluminum−nitrogen complex is approximately −54 kcal/mol, the aluminum−oxygen binding energy is approximately −34 kcal/mol, and the aluminum−fluorine on the end of the 4-fluorophenoxy ligand is approximately −8 kcal/mol, respectively, for HF/3-21G* binding energies corrected to HF/6-31G*. These values are consistent with the binding energies computed at HF/6-31G* for the $[NP(OH)_2]_3-AlF_3$ system (Table 5). The theoretical results indicate that the aluminum−nitrogen couple is strongest. However, the binding to AlF_3 continues to be strong regardless of whether or not the ring nitrogen atoms or the ligand oxygen atoms are involved.

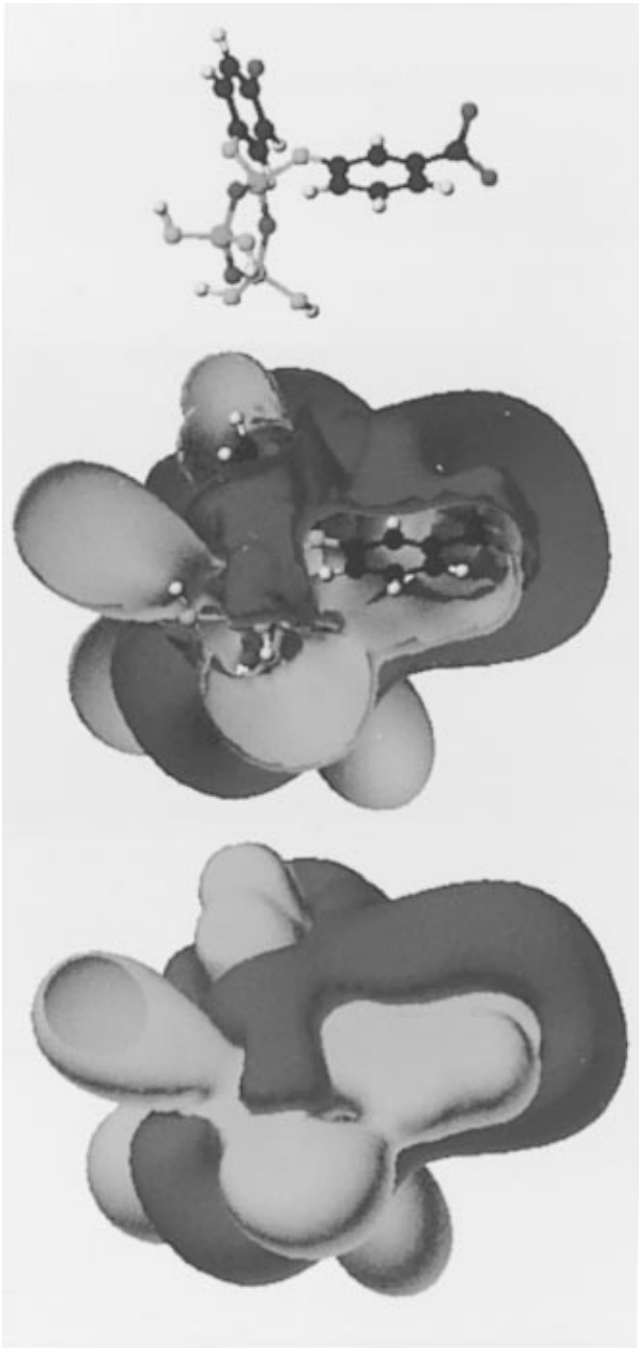

Figure 10. SCF/3-21G* electrostatic potential surface for Pre-X-1P at 6.3 kcal/mol isosurface energy. The blue regions are negative, and the red regions are positive.

X-1P: The optimized geometry for X-1P is presented in Figure 11, and the optimized parameters summarized in Table 9. The structure is fully optimized but no frequencies are computed. The geometry of the cyclotriphosphazene ring itself is very similar to $[NP(OH)_2]_3$ where the structures are similar. The N_3P_3 ring is slightly distorted from planarity, with the endocyclic dihedral angles in the ±12° range. The N−P−N and P−N−P bond angles are 113 and 127°, respectively. The computed structure for X-1P is similar to the crystal structures of phenoxy-substituted cyclotriphosphazenes.[20,21]

(20) Bandoli, G.; Casellato, U.; Gleria, M.; Grassi, A.; Montoneri, E.; Pappalardo, G. *J. Chem. Soc., Dalton Trans.* **1989**, 757.
(21) Marsh, W. C.; Trotter, J. *J. Chem. Soc. A* **1971**, 170.

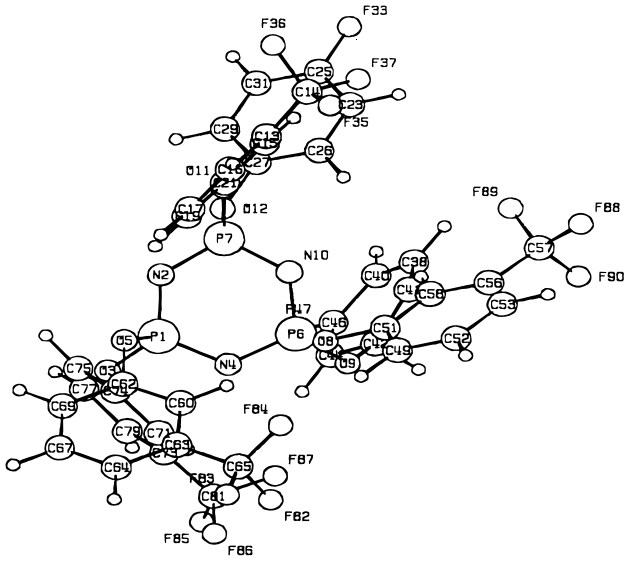

Figure 11. SCF/3-21G* optimized geometry for X-1P.

Table 9. Optimized Geometry and Bond Order (BO) for X-1P

bond	3-21G*	BO
P−N	1.575 ± 0.005	1.288 ± 0.025
P−O	1.580 ± 0.007	0.960 ± 0.024
C−C (phenyl)	1.380 ± 0.002	
C−C (CF_3)	1.490 ± 0.008	
C−F	1.352 ± 0.004	
P−N−P	126.57 ± 0.81	
N−P−N	112.73 ± 0.74	
N−P−O	110.50 ± 1.98	
O−P−O	100.84 ± 1.72	
P7−N10−P6−N4	9.21	
N10−P6−N4−P1	−16.12	
P6−N4−P1−N2	16.74	
N4−P1−N2−P7	−10.22	
P1−N2−P7−N10	4.37	
N2−P7−N10−P6	−3.91	
P−N−P−O	±(125.84 ± 13.40)	
dipole moment, D	7.34	

The molecular orbitals for X-1P are topologically similar to those presented in Figure 9 for Pre-X-1P and thus are only described here (see Figure 9). The first 12 highest occupied molecular orbitals are dominated by the phenoxy substituents, and we might expect these sites to be most accessible to chemistry. However, the endocyclic nitrogens provide strong binding to electrophiles and if sterically accessible, may well provide significant Lewis acid−base interactions. The optimized geometry in Figure 11 indicates that one of the endocyclic nitrogens, N2, is sterically accessible. While Figure 11 may well represent a local, not global minimum, the same accessibility of a ring nitrogen is evident in the crystal structure as well.[19,20] As further consideration, the electrostatic potential field surrounding X-1P is presented in Figure 12 at an isosurface energy of 18.8 kcal/mol. The regions of negative potential include the nonbonded electrons on the ring nitrogens, phenoxy oxygens and fluorines. In the optimized structure considered here (Figure 12), the negative potential due to one of the three endocyclic nitrogen atoms is clearly available to an incoming electrophile. However, an internal rotation of the ligand to another local minimum could easily deny steric access to the nitrogen atom.

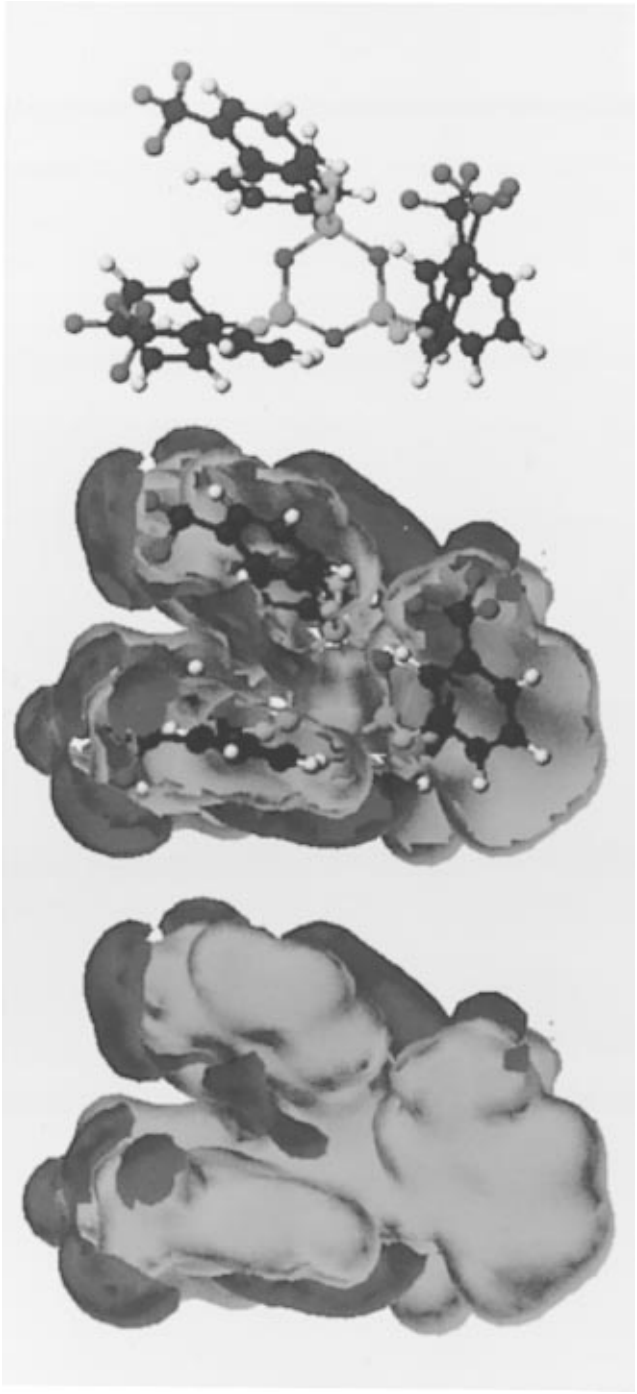

Figure 12. SCF/3-21G* electrostatic potential surface for X-1P at 18.8 kcal/mol isosurface energy. The blue regions are negative, and the red regions are positive.

Concluding Remarks

The theoretical studies presented above on cyclotriphosphazene derivatives provide us with significant insight as to how these molecules interact with electrophiles or Lewis acid sites. The theoretical results indicate that the strongest binding between X-1P and AlF_3 is realized when the endocyclic nitrogen atom bonds to the aluminum, providing a binding energy of the order of −55 kcal/mol. The magnitude of the binding energy indicates significant bonding as opposed to a dipole−dipole attraction. The lone pair of electrons on the phenoxy substituents also provide strong binding to AlF_3, although not to the extent the nitrogen atoms do, with binding energies near −37 kcal/mol. Binding to fluorine is considerably smaller, near −8 kcal/mol. The population analyses indicate that the preferred nitrogen interaction involves the p-orbital that contains the in-plane lone pair of electrons. A computed reaction coordinate with $[NPH_2]_3$ and AlF_3 gives every indication that the in-plane interaction is strongest and most stable on the potential energy surface. There is little desire on the part of the N_3P_3 ring itself to interact with Lewis acid sites parallel to the plane of the ring, i.e., with the p-orbitals housing the lone pair of electrons perpendicular to the plane of the ring. These orbitals instead provide weak π bonding with the phosphorus d-orbitals and are energetically well below the HOMO. The reason for the strong binding between AlF_3 and the ring nitrogen atom originates from the polar, almost zwitterionic character of the endocyclic P−N bond, which polarizes the nitrogen atom negatively. All data lead to the conclusion that if the ring nitrogen in X-1P is sterically accessible, this will be the preferred binding site. We also note in experimental reactions of hexaphenoxycyclotriphosphazene, sterically accessible Lewis acids such as BCl_3 preferentially bind to the ring nitrogen as compared to the exocyclic phenoxy oxygen.[22] Conversely, reactions between much larger alkyl molecules and hexaphenoxytriphosphazene preferentially bind to phenoxy groups, steric hindrance masking the stronger basicity of the endocyclic nitrogen.[23] Thus, steric accessibility will play a significant role in the interaction of X-1P to the carbon-overcoated computer disk.

Lewis acid catalysis significantly enhances the thermally induced degradation of polyperfluorinated ether lubricants. The addition of X-1P into PPFE lubricants significantly retards the degradation of PPFE.[3] Since the binding energies for perfluorinated ethers are of the order of −10 kcal/mol, the X-1P imparts protection to PPFE by preferentially interacting, and therefore passivating, the Lewis acid sites. The selective binding is based upon the strong binding energies that develop between X-1P and AlF_3.

CM9703132

(22) Horn, H. G.; Kolkmann, F. *Makromol. Chem.* **1982**, *183*, 2427.
(23) Allcock, H. R.; Levin, M. L.; Austin, P. E. *Inorg. Chem.* **1986**, *25*, 2281.